CrossMark

ORIGINAL ARTICLE

Methane reforming over Ni-based pyrochlore catalyst: deactivation studies for different reactions

Nitin Kumar[1] · Zi Wang[1] · Swarom Kanitkar[1] · J. J. Spivey[1]

Abstract A 1 wt% Ni-based $La_2Zr_2O_7$ pyrochlore catalyst was synthesized using the modified Pechini method. The catalyst was characterized by H_2-TPR, and pre- and post-reaction XRD, and tested for its methane-reforming activity under three different reaction conditions: (a) dry-reforming $(CH_4 + CO_2)$, (b) oxy-CO_2 reforming $(CH_4 + CO_2 + O_2)$, and (c) bi-reforming $(CH_4 + CO_2 + H_2O)$. The TPR results show that NiO in the fresh, calcined catalyst is completely reversible to Ni^0. The XRD results show that the crystalline pyrochlore structure is stable under all three reaction conditions. Under dry-reforming conditions, the catalyst deactivated rapidly. In oxy-reforming, the catalyst activity also decreased, but far less rapidly than under dry-reforming conditions. However, under bi-reforming conditions, no deactivation was observed at comparable times-on-stream. TPO of the spent catalysts showed greatest carbon deposition for the dry-reforming, a significant portion of which was graphitic and difficult to remove. For oxy-reforming, there was much less carbon deposition as compared to the dry-reforming, and a major part of which was the amorphous, atomic carbon, which is relatively easy to remove. Unlike under bi-reforming, no significant carbon deposition was observed at the conditions tested here. This indicates that the presence of steam resists carbon deposition compared to dry-reforming or oxy-reforming.

Graphical abstract
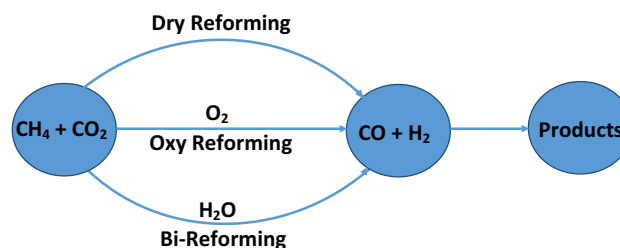
Keywords Reforming · Dry-reforming · Bi-reforming · Oxy-reforming · Pyrochlore · Syngas · Methane activation
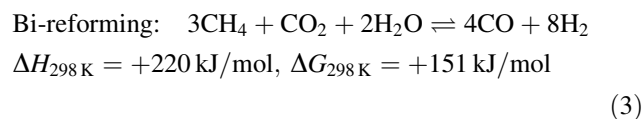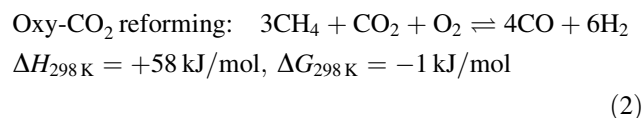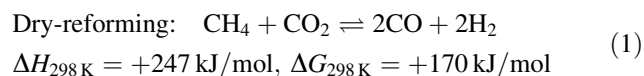
Introduction

The production of synthesis gas from methane and CO_2 is receiving significant research interest worldwide [1, 2]. Methane and CO_2 are the main components of some natural gas resources, including coalbed gases, and are potential large sources of energy. The production of these gases is predicted to increase in the near future [3]. The conversion of methane and CO_2 to syngas requires demanding conditions, e.g., temperatures above ~ 800 °C, making it even more important to efficiently convert these gases into useful products using stable, active catalysts.

Many different reactions are studied that utilize both CH_4 and CO_2, but the most viable option is the catalytic conversion of these gases to produce syngas, a mixture of CO and H_2 [4]. Syngas can be used to produce a range of high-value chemicals, such as methanol, higher oxygenates, and Fischer–Tropsch products [5–8]. Some of the

✉ J. J. Spivey
   jjspivey@lsu.edu

[1] Louisiana State University, Baton Rouge, LA 70803, USA

مدينة الملك عبدالعزيز
KACST للعلوم والتقنية

Springer

options available for direct conversion of these gases to produce syngas are given below:

Dry-reforming: $CH_4 + CO_2 \rightleftharpoons 2CO + 2H_2$
$\Delta H_{298\,K} = +247\,kJ/mol,\ \Delta G_{298\,K} = +170\,kJ/mol$ (1)

Oxy-CO_2 reforming: $3CH_4 + CO_2 + O_2 \rightleftharpoons 4CO + 6H_2$
$\Delta H_{298\,K} = +58\,kJ/mol,\ \Delta G_{298\,K} = -1\,kJ/mol$ (2)

Bi-reforming: $3CH_4 + CO_2 + 2H_2O \rightleftharpoons 4CO + 8H_2$
$\Delta H_{298\,K} = +220\,kJ/mol,\ \Delta G_{298\,K} = +151\,kJ/mol$ (3)

Dry-reforming produces a syngas with 1/1 H_2/CO ratio, and therefore, extra H_2 must be added for the downstream Fischer–Tropsch or methanol synthesis. One of the challenges associated with dry-reforming is that of the carbon deposition, which typically results in the severe, rapid deactivation [9]. Oxy-CO_2 reforming, on the other hand, is much less endothermic compared to the dry-reforming, which could result in significant energy savings. However, severe temperature gradients within the catalyst bed can deactivate the catalyst, especially for the scaled-up systems. The syngas produced in oxy-reforming also falls short of the desired 2/1 H_2/CO ratio. The bi-reforming reaction, although highly endothermic, results in the desired 2/1 H_2/CO ratio, and the process can be directly coupled with the downstream F–T or methanol synthesis processes.

All technologies to reform CH_4 and CO_2 directly to syngas face with several challenges. These challenges arise mainly due to the highly endothermic nature of the reaction itself, which requires high temperatures (~ 800 to $1000\,^\circ C$) to reach high equilibrium conversions. At these conditions, many catalysts are not thermally stable as a result of sintering or collapse of the crystal structure. Another major problem is due to carbon deposition, which results in deactivation. Therefore, the reforming catalyst should meet these important criteria: (a) thermal stability of the support, (b) resistance to sintering of the active metal, (c) resistance to carbon deposition, and (d) high activity with time-on-stream to reach equilibrium conversions.

One approach is to add active metals to a thermally stable crystalline oxide, such as a pyrochlore, as has been shown to be promising for dry-reforming [9–12]. Pyrochlores are highly crystalline defect fluorite oxide with the general formula of $A_2B_2O_7$, where A is a lanthanide series element, and B is a transition metal, and the ionic ratio of r_A/r_B is 1.4–1.6. They have proven high temperature stability in various applications, such as gas turbine thermal barrier coatings [13], but have only recently been investigated as catalysts. The pyrochlore structure, if properly synthesized, can incorporate active metals, such as Ni, at low loadings. This provides a strong interaction between the active metal and the support, which can significantly improve the coke resistance of the catalyst [14]. The first use of pyrochlore as catalysts was by Ashcroft et al. [15], where they tested the structure with several active metals. However, their pyrochlore structure collapsed at dry-reforming conditions at 660 °C.

In the present work, a Ni-based pyrochlore having $La_2Zr_2O_7$ was synthesized by modified Pechini method [16, 17] and characterized using TPR/TPO and XRD. The catalyst was tested under three reforming reaction conditions at a reference temperature of 750 °C: (a) dry-reforming (reaction 1), (b) oxy-reforming (reaction 2), and (c) bi-reforming (reaction 3). The spent catalyst from each reaction was characterized using temperature program oxidation (to investigate carbon deposition) and XRD (to investigate any structural changes).

Experimental

Catalyst preparation

The 1 % LNZ pyrochlore catalyst was prepared using a modified Pechini method. The preparation method produces highly uniform crystallites and is explained in detail elsewhere [12, 16–21]. The precursors used for La, Ni, and Zr were lanthanum nitrate [$La(NO_3)_3 \cdot 6H_2O$], nickel nitrate [$Ni(NO_3)_2 \cdot 6H_2O$], and zirconium nitrate [$ZrO(NO_3)_2 \cdot nH_2O$], respectively. The nitrate salts were separately dissolved in deionized water and then mixed with a citric acid (CA) solution in a molar ratio of CA:metal = 1.2:1. The solution was continuously stirred and heated to 75 °C to ensure complete metal complexation. At 75 °C, a 1:1 molar ratio of ethylene glycol (EG) to CA was added to the solution. The solution was kept stirred on the hot plate until most of the water had evaporated and a transparent, viscous gel was obtained. After this the stirring was stopped and the gel was left on the hot plate to promote the polyesterification reaction between EG and CA to form an organic polymeric network. The nitrate precursors started to decompose at this condition, which was evident from the large plumes of NO_x and bubbling in the gel. The resulting foam-like mixture was placed in an oven at 110 °C to dry overnight. The mixture was then calcined at 1000 °C for 8 h to oxidize the organic precursors and form the pyrochlore catalyst.

Temperature-programmed reduction (TPR)

Temperature-programmed reduction (TPR) profiles of the calcined catalyst were recorded using an Altamira AMI

200 unit equipped with a thermal conductivity detector (TCD) [21]. 50 mg of catalyst sample was first oxidized in a fixed-bed micro-reactor system under flowing 5 % O_2/He at 950 °C. It was then cooled to 25 °C under helium flow. TPR was performed using a 10 % H_2/Ar mixture at a flow rate of 50 cm^3/min, while the temperature was linearly ramped from 25 to 950 °C at 10 °C/min. The catalyst was then cooled to 25 °C under helium flow and, then, again oxidized under 5 % O_2/He at 950 °C. The catalyst was again cooled back to 25 °C under helium flow. A second TPR was carried out under the same conditions as that of the first TPR mentioned above.

X-ray diffraction

X-ray diffraction (XRD) experiments were carried out using Empyrean X-ray diffractometer (PANalytical) using Cu K_α radiation ($\lambda = 1.5406$ Å). The scan angle was varied from 0 to 90° with a step size of 0.017°. Data analysis was done using the software X'Pert HighScore Plus (v3.0).

Equilibrium calculations

Thermodynamic equilibrium calculations were carried out using HSC Chemistry 8.0 (Outotec, Finland), which uses Gibbs free energy minimization for all the components at a given condition. Molar ratios of the feeds were taken to be the same as their stoichiometric ratios corresponding to each reaction, and calculations were carried out for all the three reaction systems: dry-reforming, oxy-reforming, and bi-reforming. Products allowed to form in the simulation were carbon, CO, and H_2. Equilibrium calculations were carried out at 1 atm pressure, and the amount of carbon formed for all three reaction systems at different temperatures was calculated. The amount of carbon was normalized with respect to the total carbon entering in each of the reactions so as to compare them on the same basis.

Catalyst activity test

Catalytic activity tests were carried out in a ¼″ size fixed-bed reactor made of quartz, which can withstand up to 1200 °C under 1 atm [21]. The experiments were carried out in an AMI 200 unit (Altamira Instruments, Pittsburgh, PA). The reactor is equipped with a thermocouple that is inserted directly into the catalyst bed to measure the actual temperature of the catalyst. Both ends of the catalyst bed were plugged with quartz wool to avoid entrainment of any catalyst particles with the gas stream. Before the reaction, the catalyst was pretreated with 10 % O_2/He flow at a temperature of 800 °C followed by cooling down to room temperature under pure helium. The catalyst was then reduced under 10 % H_2/He flow at 800 °C. After the

Table 1 Mole% of feeds used for various reactions on a helium-free basis

Reaction	CO_2 (mol%)	CH_4 (mol%)	O_2 (mol%)	H_2O (mol%)
Dry-reforming	50	50	–	–
Oxy-reforming	20	60	20	–
Bi-reforming	16	51	–	33

reduction, the catalyst was cooled to the reaction temperature under helium flow.

The gases used for the reactions were 10 % CO_2/He, 10 % CH_4/He, and 10 % O_2/He. All the experiments were carried out at 1 atm pressure and space velocities in the range of 96,000–100,000 scc h^{-1} g cat^{-1}. The molar ratios of various gases used for different reactions on a helium free basis are shown in Table 1. The experimental molar ratios were kept close to the stoichiometric ratios corresponding to different reactions.

For the bi-reforming reaction, water was fed to the reactor at a controlled rate using a HPLC pump [21]. The water flows through a vaporizer where steam is formed, which is later mixed with other gases before flowing through the catalyst bed. All the inlet and outlet lines were heat-traced to 200 °C to avoid condensation of steam. Outlet gases were analyzed using an inline quadrupole mass spectrometer.

A temperature program oxidation (TPO) was carried out on the spent catalyst after each reaction. For TPO, the catalyst was heated from room temperature to 950 °C under 10 % O_2/He mixture at a ramp rate of 10 °C/min, and CO_2 signal (mass 44) was recorded in a mass spectrometer.

Results and discussion

Temperature-programmed reduction

The TPR results are shown in Fig. 1 [21]. The two curves represent two consecutive TPRs with an intermittent oxidation step. These two consecutive TPRs were carried out to investigate whether the catalyst retains its structure in the second TPR after the high temperature treatment in the first TPR. Figure 1 shows that these two successive TPR profiles are fully reproducible, indicating that the reduction of NiO and oxidation of metallic Ni are completely reversible. There is no detectable change in the structure of the catalyst or any sintering of the metal as a result of the 950 °C TPR/TPO.

Figure 1 also shows the reduction of nickel oxide under four different peaks. The peak at 305 °C can be attributed to the reduction of bulk NiO [22, 23]. The peaks at 352 °C
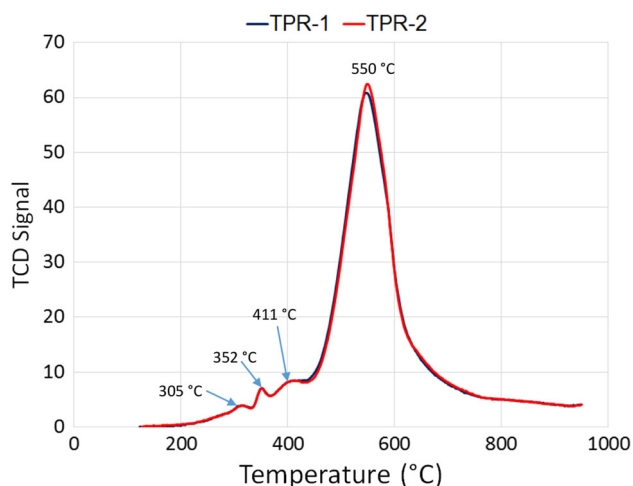
Fig. 1 Temperature program reduction results for 1 % LNZ catalyst [21]. The *two curves* represent two consecutive TPRs with an oxidation step in-between

Fig. 2 XRD patterns for 1 % LNZ catalyst. **a** Fresh calcined 1 % LNZ, **b** 1 % LNZ after dry-reforming reaction, **c** 1 % LNZ after oxy-reforming reaction, and **d** 1 % LNZ after bi-reforming reaction

and 411 °C can be assigned due to the sequential reduction of Ni^{3+} to Ni^{2+} and Ni^{2+} to Ni^{0}, respectively [24]. Finally, most of the nickel in the catalyst is reduced under the peak at 550 °C, which can be attributed to the reduction of highly dispersed NiO species interacting strongly with the support [25]. This indicates that most of the Ni in the catalyst is present in a highly dispersed form, strongly interacting with the pyrochlore support.

X-ray diffraction (XRD)

The XRD results for fresh 1 % LNZ and spent catalysts from the three reactions are shown in Fig. 2. Figure 2a shows the XRD patterns for fresh calcined catalyst. Figure 2b–d shows the XRD patterns for spent catalysts obtained after dry-reforming, oxy-reforming, and bi-reforming reactions, respectively.

Figure 2 shows that there is no change in the peak ratios or positions for the fresh and spent catalysts from any of the three reactions, which indicates that the crystalline structure of the catalyst does not change under any of the reforming conditions. All the peaks seen in Fig. 2 correspond to that of the $La_2Zr_2O_7$ phase, and no peaks corresponding to NiO or metallic Ni phases are observed. This is due to low metal loading and high dispersion of Ni in the catalyst. These results also support the argument that the pyrochlore structure is unaffected as a result of reforming at high temperatures under different feed conditions. Pyrochlore catalysts containing rare earth metals have been used by Ashcroft et al. [15] to study dry-reforming, but their structure was not stable and they observed a breakdown of the pyrochlore structure during the dry-reforming at 660 °C. In our case, on the other hand, the XRD patterns for spent catalysts after dry-, oxy-, and bi-reforming
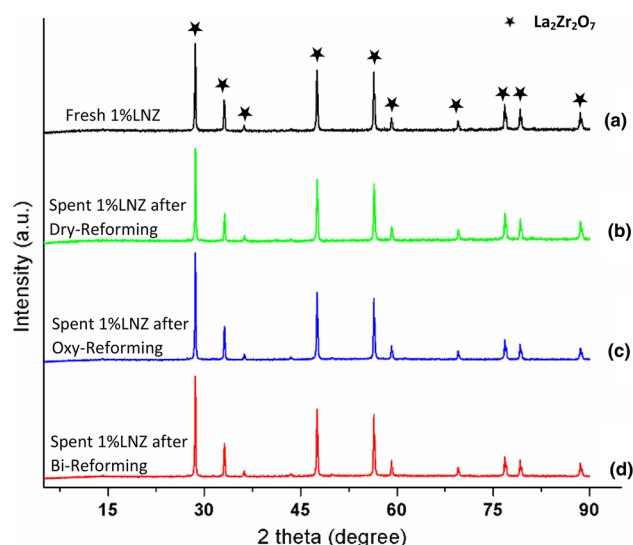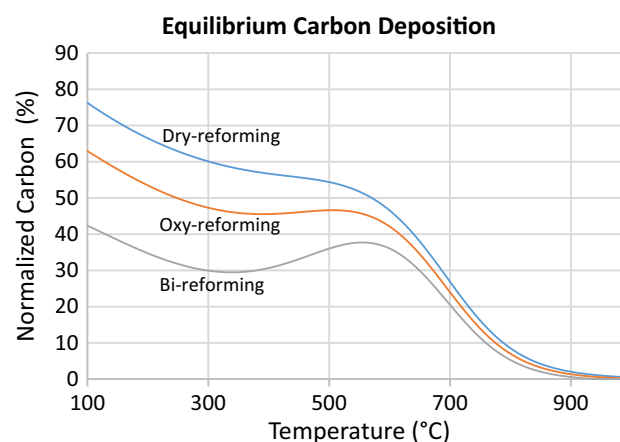

Fig. 3 Equilibrium carbon deposition for the *three* reactions calculated at atmospheric pressure and different temperatures using HSC Chemistry. The molar ratios of feeds were taken corresponding to the stoichiometry of the three reforming reactions

conditions were not changed when compared to that of the fresh catalyst, indicating high thermal resistance of the catalyst under the three reforming conditions studied here.

Thermodynamic analysis of carbon deposition

The equilibrium carbon deposition corresponding to each reaction was calculated at different temperatures, and the results are shown in Fig. 3.

Figure 3 shows that there is a significant thermodynamic driving force for carbon formation at temperatures below ~800 °C for all three reactions, with the following trend:
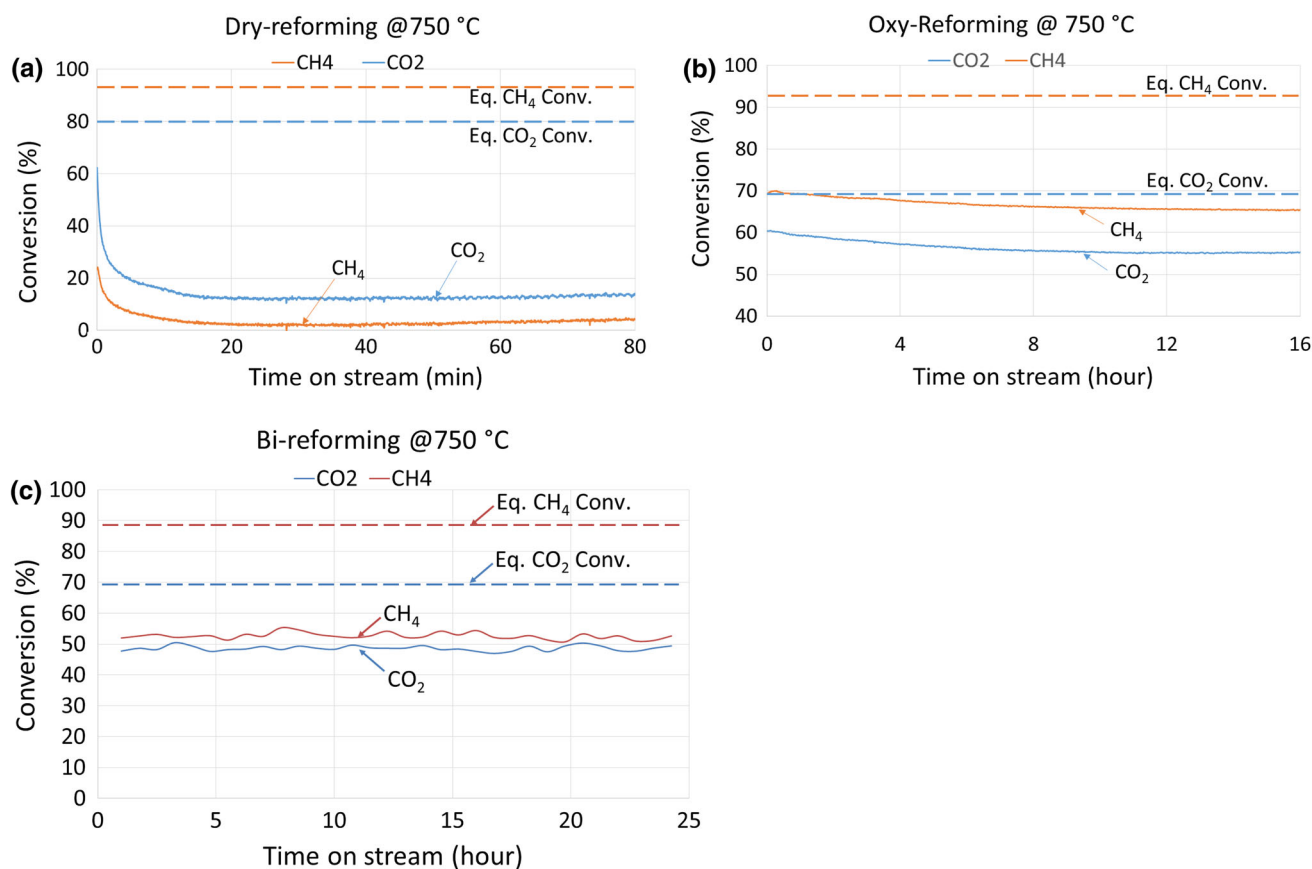
Fig. 4 Time-on-stream tests for 1 % LNZ catalyst at 750 °C for **a** dry-reforming, **b** oxy-reforming, **c** bi-reforming. The feed compositions for each reaction were taken as shown in Table 1. *Broken lines* represent the equilibrium conversions corresponding to each conditions

Dry-reforming > oxy-reforming > bi-reforming

The carbon deposition is thermodynamically least favorable in the case of bi-reforming, as compared to the other two reforming conditions. However, kinetics can limit the carbon-removal reactions, and carbon formation could be significant, even at high temperatures [3].

Catalyst activity with time-on-stream

The activity of 1 % LNZ catalyst with time-on-stream at 750 °C is plotted in Fig. 4 for all three reforming reactions. The inlet feed was fixed for each reaction as shown in Table 1. Note that the equilibrium conversions in Fig. 4a–c differ for each of the three reforming reactions due to different stoichiometric feed concentrations.

Rapid deactivation of 1 % LNZ catalyst is clearly seen under dry-reforming conditions. For oxy-reforming, the catalyst is much more resistant to deactivation as compared to dry-reforming. For the bi-reforming, however, the catalyst does not deactivate for at least 24 h time-on-stream at 750 °C. As judged by the CH_4 and CO_2 conversions, bi-reforming conditions produce the most stable syngas product on this 1 % LNZ catalyst.

It has been reported [26–30] that the presence of oxidizing agents, such as O_2 or H_2O, can minimize the surface carbon deposition in methane reforming. The mechanism of carbon removal is generally thought to be due to the oxidation of the carbon precursor species [partially dehydrogenated CH_x species and/or $C_{(s)}$] in the presence of oxidizing agents, such as O_2 or H_2O [26]. For the work reported here, this is why the carbon formation is limited for the 1 % LNZ catalyst in the presence of an oxidizing agent, e.g., O_2 in oxy-reforming and H_2O in bi-reforming.

Carbon deposition studies

The carbon deposition was studied using temperature program oxidation (TPO) for the spent catalysts from all three reactions.

Figure 5 shows three distinct TPO peaks for the spent catalyst from dry-reforming. The peak at 450 °C can be assigned due to amorphous, atomic carbon, C_α, which can be relatively easily gasified [3, 31, 32]. Peak at 626 °C could be due to the polymeric carbon, C_β, which can form as a result of rearrangement of the C_α carbons and is relatively less reactive. Finally, the peak at 717 °C can be

Fig. 5 Temperature program oxidation results for spent catalysts from different reactions
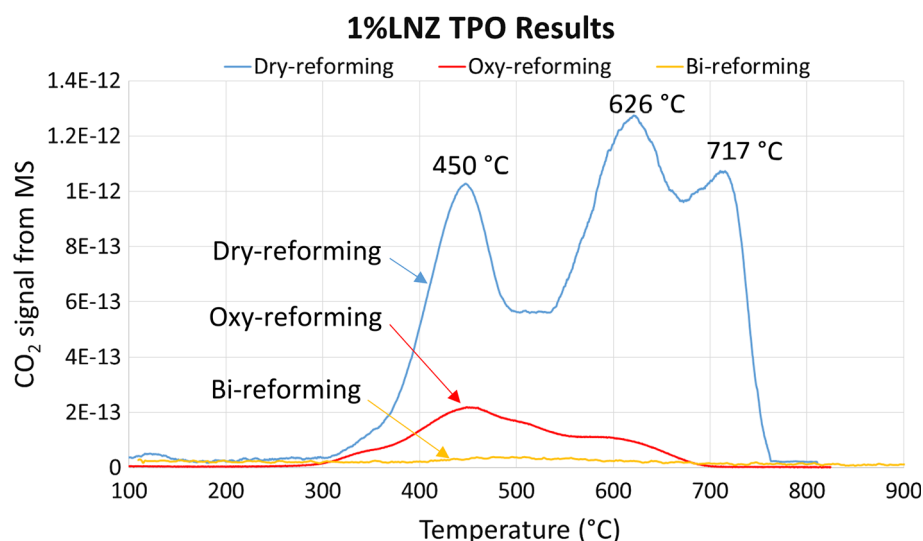
assigned due to the formation of carbon filaments or graphitic form of carbon, also known as 'whiskers' [14, 32, 33]. These whiskers are mechanically very strong and can permanently deactivate the catalyst.

For the spent catalyst from oxy-reforming, only peaks corresponding to C_α and C_β are observed, and no graphitic carbons are present. The less reactivity, and less amount of carbon in oxy-reforming compared to dry-reforming is clearly the reason that there is far less deactivation in oxy-reforming than in dry-reforming (Fig. 4a, b). For example, this is also evident from the fact that the C_β peak is much smaller in area compared to that of the C_α peak for the oxy-reforming reaction. This is not the case with the dry-reforming reaction, where C–C chain growth is pronounced for the carbon deposition, leading to the formation of refractory graphitic carbon. For the spent catalyst after the bi-reforming reaction, however, no significant amount of carbon is observed in the TPO, indicating that steam in the reactants appears to react more rapidly with the surface carbon than under oxy-reforming conditions.

The activity of the catalyst with time-on-stream for these reactions (Fig. 4) can be directly correlated to the amount of carbon deposited on the active sites of the catalyst. A rapid decrease in the catalytic activity under dry-reforming conditions is due to excessive carbon deposition under more highly reducing conditions of dry-reforming compared to the other reforming conditions. The far less rapid decrease in activity with time-on-stream for the oxy-reforming reaction (Fig. 4b) is directly related to far less amount (and far less reactive) of carbon deposited on the catalyst, as seen in Fig. 5.

Finally, the lack of any significant deactivation under bi-reforming conditions can be attributed to the lack of any significant carbon deposition. The carbon depositions for the spent catalysts from all three reactions are consistent

and directly attributable to their deactivation. These results are also consistent with the thermodynamics of carbon deposition as shown in Fig. 3.

Conclusions

One wt% Ni-doped with $La_2Zr_2O_7$ pyrochlore catalyst has been tested in three types of methane reforming reaction conditions. The pyrochlore crystalline structure is stable at these demanding conditions, as indicated by XRD. Under dry-reforming and oxy-reforming conditions, carbon deposition appears to be directly and solely responsible for deactivation. Carbon deposition is far more extensive in dry-reforming than other conditions. However, no observable carbon is found under bi-reforming conditions. There is no evidence in XRD or TPR that nickel sinters or causes deactivation.

The presence of an oxidizing agent, such as O_2 in the case of oxy-reforming and steam in the case of bi-reforming, significantly reduces the deactivation compared to dry-reforming. Steam in the inlet (i.e., in bi-reforming) appears to oxidize carbon or its precursors, with no measurable deactivation over a 24-h period.

References

1. Raju ASK, Park CS, Norbeck JM (2009) Synthesis gas production using steam hydrogasification and steam reforming. Fuel Process Technol 90(2):330–336
2. Gangadharan P, Kanchi KC, Lou HH (2012) Evaluation of the economic and environmental impact of combining dry reforming with steam reforming of methane. Chem Eng Res Des 90(11):1956–1968
3. Kumar N, Shojaee M, Spivey JJ (2015) Catalytic bi-reforming of methane: from greenhouse gases to syngas. Curr Opin Chem Eng 9:8–15
4. York AE, Xiao T, Green MH (2003) Brief Overview of the Partial Oxidation of Methane to Synthesis Gas. Top Catal 22(3–4):345–358
5. Kumar N, Smith ML, Spivey JJ (2012) Characterization and testing of silica-supported cobalt-palladium catalysts for conversion of syngas to oxygenates. J Catal 289:218–226
6. Kumar N, Payzant EA et al (2011) Combined in situ XRD and in situ XANES studies on the reduction behavior of a rhenium promoted cobalt catalyst. Phys Chem Chem Phys 13(32):14735–14741
7. Kumar N et al (2011) In Situ FT-IR Study on the Effect of Cobalt Precursors on CO Adsorption Behavior. J Phys Chem C 115(4):990–998
8. Spivey JJ, Egbebi A (2007) Heterogeneous catalytic synthesis of ethanol from biomass-derived syngas. Chem Soc Rev 36(9):1514–1528
9. Pakhare D, Spivey J (2014) A review of dry (CO_2) reforming of methane over noble metal catalysts. Chem Soc Rev 43(22):7813–7837
10. Pakhare D, Wu H et al (2013) Characterization and activity study of the Rh-substituted pyrochlores for CO_2 (dry) reforming of CH_4. Appl Petrochem Res 3(3–4):117–129
11. Pakhare D, Haynes D et al (2012) Role of metal substitution in lanthanum zirconate pyrochlores ($La_2Zr_2O_7$) for dry (CO_2) reforming of methane (DRM). Appl Petrochem Res 2(1–2):27–35
12. Gaur S, Haynes DJ, Spivey JJ (2011) Rh, Ni, and Ca substituted pyrochlore catalysts for dry reforming of methane. Appl Catal A 403(1–2):142–151
13. Ramachandran CS, Balasubramanian V, Ananthapadmanabhan P (2013) Thermal cycling behaviour of plasma sprayed lanthanum zirconate based coatings under concurrent infiltration by a molten glass concoction. Ceram Int 39(2):1413–1431
14. Liu C-J, Ye J et al (2011) Progresses in the Preparation of Coke Resistant Ni-based Catalyst for Steam and CO_2 Reforming of Methane. Chem Cat Chem 3(3):529–541
15. Ashcroft AT, Cheetam AK et al (1992) An in situ study of pyrochlore-type catalysts for the formation of synthesis gas from methane and carbon dioxide. R Soc Chem 114:184–189 (Catalysis and Surface Characterisation)
16. Pechini PM (1967) Method of preparing lead and alkaline earth titanates and niobates and coating method using the same to form a capacitor. In: Patents U (ed). Sprague Electric Co, USA
17. Haynes DJ, Berry DA et al (2008) Catalytic partial oxidation of n-tetradecane using pyrochlores: effect of Rh and Sr substitution. Catal Today 136(3–4):206–213
18. Tietz F, Schmidt A, Zahid M (2004) Investigation of the quasi-ternary system LaMnO3-LaCoO3-"LaCuO3"-I: the series La(Mn0.5Co0.5)1-xCuxO3-δ. J Solid State Chem 177(3):745–751
19. Majid A, Tunney J et al (2005) Preparation of SrFeO∼2.85 perovskite using a citric acid assisted Pechini-type method. J Alloys Compd 398(1–2):48–54
20. Lepe FJ, Fernández-Urbán J et al (2005) Synthesis and electrical properties of new rare-earth titanium perovskites for SOFC anode applications. J Power Sources 151:74–78
21. Kumar N, Roy A et al (2016) Bi-reforming of methane on Ni-based pyrochlore catalyst. Appl Catal A 517:211–216
22. Bai CS, Soled S et al (1992) The preparation and characterization of the phases formed by the reactions of nickel and lanthanum nitrates with magnesium aluminate. J Solid State Chem 100(2):307–312
23. Rodulfo-Baechler SA, Pernía W et al (2006) Influence of lanthanum carbonate phases of Ni/La0.98Sr0.02O x catalyst over the oxidative transformation of methane. Catal Lett 112(3–4):231–237
24. Sania Maria de Lima, Assaf JM (2002) Synthesis and Characterization of LaNiO3, LaNi(1-x)FexO3 and LaNi(1-x)CoxO3 Perovskite Oxides for Catalysis Application. Mater Res 5(3):329–335
25. Mile B, Stirling D et al (1988) The location of nickel oxide and nickel in silica-supported catalysts: two forms of "NiO" and the assignment of temperature-programmed reduction profiles. J Catal 114(2):217–229
26. Choudhary VR, Mondal KC (2006) CO_2 reforming of methane combined with steam reforming or partial oxidation of methane to syngas over NdCoO3 perovskite-type mixed metal-oxide catalyst. Appl Energy 83(9):1024–1032
27. Choudhary VR, Mondal KC, Choudhary TV (2006) Oxy-CO_2 reforming of methane to syngas over CoOx/MgO/SA-5205 catalyst. Fuel 85(17–18):2484–2488
28. Choudhary VR, Mondal KC, Choudhary TV (2006) Oxy-CO_2 Reforming of Methane to Syngas over CoOx/CeO2/SA-5205 Catalyst. Energy Fuels 20(5):1753–1756
29. Choudhary VR, Rajput AM (1996) Simultaneous Carbon Dioxide and Steam Reforming of Methane to Syngas over NiO-CaO Catalyst. Ind Eng Chem Res 35(11):3934–3939
30. Choudhary VR, Uphade BS, Mamman AS (1998) Simultaneous steam and CO_2 reforming of methane to syngas over NiO/MgO/SA-5205 in presence and absence of oxygen. Appl Catal A 168(1):33–46
31. Itkulova SS, Zakumbaeva GD et al (2014) Syngas production by bireforming of methane over Co-based alumina-supported catalysts. Catal Today 228(0):194–198
32. Trimm DL (1997) Coke formation and minimisation during steam reforming reactions. Catal Today 37(3):233–238
33. Snoeck JW, Froment GF, Fowles M (2002) Steam/CO_2 Reforming of Methane. Carbon Filament Formation by the Boudouard Reaction and Gasification by CO_2, by H_2, and by Steam: Kinetic Study. Ind Eng Chem Res 41(17):4252–4265